Study on measurement of medium and low spatial wavefront errors of long focal length lens

Chunxiang Jin (金春祥)[1,2], Shijie Liu (刘世杰)[1*], You Zhou (周 游)[1], Xueke Xu (徐学科)[1], Chaoyang Wei (魏朝阳)[1], and Jianda Shao (邵建达)[1]

[1]*Shanghai Institute of Optics and Fine Mechanics, Chinese Academy of Sciences, Shanghai 201800, China*

[2]*University of the Chinese Academy of Sciences, Beijing, 100039, China*

[*]*Corresponding author: shijieliu@siom.ac.cn*

Received March 24, 2014; accepted May 3, 2014; posted online November 3, 2014

High-power laser system has a requirement for the medium and low spatial wavefront errors of the transmitted wavefront of the spatial filter, which is a spherical lens with long focal length (> 10 m) and large aperture (> 400×400 (mm)). Two interferometric methods are analyzed and compared for testing the medium and low spatial wavefront errors of the long focal length lens with an instantaneous interferometer, using large aperture plane mirror and concave mirror as retroflectors, respectively. The two kinds of beam path arrangements are designed using ray tracing method. Wavefront aberration and modulation transfer function are used as merit functions. The reason for their different ability to test the wavefront is also analyzed. To evaluate the feasibility of test methods, tolerances analyses are performed to determine the tolerances demanding the fabrication and assembly of each optical element. It is proved that a relatively short optical path with a large aperture concave mirror is satisfied for testing the medium and low spatial wavefront errors of the transmitted wavefront of the spatial filter.

OCIS codes: 120.3620, 120.3688, 110.1758.

doi: 10.3788/COL201412.S21203.

Testing the transmitted wavefront of long focal length lens has always been a difficult problem, especially when the lens's aperture is large. High-power laser system has a requirement for the medium and low spatial wavefront errors of the transmitted wavefront of the spatial filter, which is a spherical lens with long focal length (>12 m) and large aperture (>400×400 (mm))[1]. The low-frequency (<0.03 cycles/mm) wavefront distortion determines the shape of the focal spot, while the medium frequency (0.03–8.3 cycles/mm) wavefront error produces wings of the focal spot and self-focusing damage[2]. Power spectrum density (PSD) is used to characterize the medium frequency wavefront error, and in this article, we focus on PSD1 (0.03–0.4 cycles/mm). In order to reduce the middle and low spatial wavefront errors of the lens, it is necessary to establish a test method for medium and low-frequency wavefront errors to guide the machining process. There are many means for inspecting low spatial wavefront error, but to the best of our knowledge, few works have been found on testing the medium spatial wavefront error of such long focal length lens with large aperture.

On testing the wavefront error of the long focal length lens, some methods have been developed based on Shack–Hartmann wavefront sensor (SHWFS)[3,4] or Talbot effect and Moire technique[5,6]. Both the methods inspect the wavefront slope of some number of points on the wavefront discretely, which limit the spatial frequency bandwidth they can test. For a SHWFS consisting of 32×32 (μm) lens, if the aperture of tested lens is 500×500 (mm)[4,7], the highest spatial frequency can be tested is less than the Nyquist sample frequency which is 32/500 mm/2 = 0.032 cycles/mm. So PSD1 (0.03–0.4 cycles/mm) cannot be inspected. As a result, both methods can test low-order figure, but cannot inspect medium spatial wavefront error of the whole range of PSD1. Phase shifting interferometry is also used to test wavefront error of the long focal length lens[8]. Medium spatial wavefront error can be inspected because of the high resolution of the CCD of the interferometer. To match the *F*-number of the lens under test, a long optical path is needed. As a result, the air turbulence and vibration of the test platform will affect the interferogram fringes and reduce the accuracy of the results. Modern instantaneous interferometry with carrier fringe method is capable of testing the surface or wavefront of optical element by capturing one piece of interferogram with high-speed camera. Consequently, it can work in unsteady environment with air turbulence and platform vibration. So it is necessary to develop a new method to test medium and low spatial wavefront errors of long focal length lens with dynamic interferometer.

Theoretically, the spatial frequency bandwidth, which the interferometer can test is proportional to the aperture of stop L_0 and the size of inspector array N[9]. The resolution of the CCD of Zygo dynamic interferometer is 1024×1024. Suppose the aperture of the tested lens is 500×500 (mm), then the sample spatial frequency $f_1 = N/L_0 = 1024/500 = 2.048$ cycles/mm. According to the Nyquist sample theory, the Nyquist sample frequency f_{max} is half of f_1 to recover the original information completely, that is, equal to 1.024 cycles/mm.

 © 2014 Chinese Optics Letters

The lowest spatial frequency $f_0 = 1/L_0$. In the light of the method provided by Church[10], the effective spatial frequency bandwidth of interferometer is estimated as

$$2f_0 < f < f_{max}/2. \quad (1)$$

Therefore, the lowest spatial frequency tested by the dynamic interferometer is $2f_0 = 0.004$ cycles/mm, and the highest spatial frequency is $f_{max}/2 = 0.512$ cycles/mm which cover the range of PSD1(0.03–0.4 cycles/mm). The Zygo DynaFiz instantaneous interferometer is used for inspecting the middle spatial wavefront error (PSD1) over the entire aperture.

The requirement for the transmitted wavefront of the spatial filter is less than 1/3λ in Peak To Valley (PV). The main aberration generated by the large aperture lens in the interferometric path is spherical aberration, which is proportional to the aperture of lens squared, so the larger the lens' aperture, the greater the spherical aberration[11]. In order to eliminate the spherical aberration, compensated lens is needed to reduce the wavefront slope and fringes in interferogram to extract the wavefront error wanted[12].

Using a large aperture plane mirror to reflect the test light back into the test system is cost-effective, compared with large aperture concave mirror because large plane mirror is more easily fabricated using continuous polishing technology. Besides, we can directly use the high-quality plane retroreflector of Φ600 mm plane interferometer in our laboratory. So, a test plan with plane mirror as reflector is designed. Figure 1 shows the simplified schematic of the beam path of test plan with plane mirror. The aperture of the first compensated lens is related to the distance from the tested lens to compensated lens shown in

$$\frac{d}{D} = \frac{F-L}{F}, \quad (3a)$$

$$d = D^*\left(1-\frac{L}{F}\right), L = F^*\left(1-\frac{d}{D}\right). \quad (3b)$$

When $D = 600$ mm and $F = 11805$ mm

$$d = 600^*\left(1-\frac{L}{11805}\right). \quad (3c)$$

Equation (3c) illustrates that it is impossible to maintain short total length of the test system and small aperture compensated lens at the same time. Compensated lens close to the tested lens has more powerful ability to eliminate the spherical aberration generated by the large aperture of the long focal length lens. In consideration of the assembly of the optical components, the compensated lenses will be clamped in a lens cone, and the exit pupil of the compensated group should be equal to the aperture of the interferometer (100 mm). As a result, the aperture of the compensated lens should not be > 200 mm due to the restriction of the clamping device of lenses. So it can be computed that the shortest test distance is 7870 mm, while the aperture of compensated lens is 200 mm. Here we use the Zygo DynaFiz interferometer with a standard plane lens (Φ100 mm), so the compensated lens should be a negative lens to transform the plane wave from the interferometer to a diverging spherical wave. Suppose the focal length of the tested lens is 12 m. With the help of optical design software Zemax, Fig. 2 illustrates the beam path diagram of the test system with a piece of compensated lens and a large aperture plane reflector. Lens data are shown in Table 1. The total length of the optical path is 10085 mm.

The requirement of the transmitted wavefront is PV < 1/3λ, PV of the wavefront of the test system is 0.1363λ, and RMS 0.0254λ (Fig. 3), and modulation transfer function (MTF) of the test system is > 0.95 over middle and low spatial frequencies, as shown in Fig. 4. Hence, the design before tolerances analyses is up to specification of the test requirements.

Another optical test plan is designed in order to shorten the total optical path and reduce the influence of environment disturbance. Because the back surface of the tested lens is convex sphere, concave mirror is more suitable in the interferometric path. On one hand, the concave mirror is more capable of eliminating the negative spherical aberration generated by the positive lens under test than plane reflector. On the other hand, the concave mirror well fits the figure of the wavefront of the diverging light transmitted by the lens under test. As a result, the test light can be reflected back into the interferometer in autocollimating arrangement in a relatively short optical path.

Compensated lenses consist of two spherical lenses which are inserted into the optical path to shorten the total optical length and eliminate the spherical aberration generated by the long focal length lens. The plane wave from the Zygo DynaFiz interferometer is refracted by compensated lens and the long focal length lens,

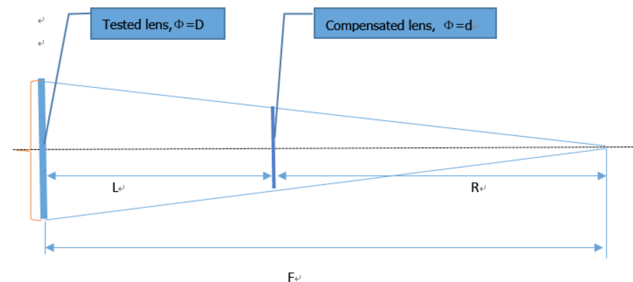

Fig. 1. Schematic of simplified beam path diagram with plane mirror.

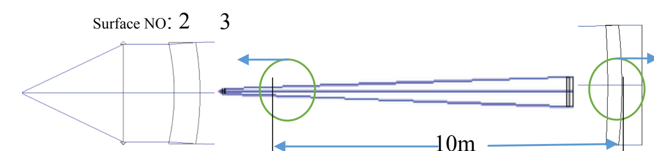

Fig. 2. Layout of the beam path of the test system with plane mirror.

Table 1. Lens Data of the Test System with Plane Mirror (units: mm)

	Surf:Type	Radius	Thickness	Glass	Semi-Diameter
OBJ	Standard	Infinity	100.000000		0.000000
STO	Paraxial		50.000000		48.000000
2	Standard	364.304151	20.000000	H-K9L	48.000000
3	Standard	261.935327	9745.870522		47.044996
4	Standard	-5000.000000	70.000000	H-K9L	297.567113
5	Standard	-2758.000000	100.000000		299.898721
6	Standard	Infinity	–100.000000 p	Mirror	299.898550

and then reflected back into the interferometer by a large aperture concave mirror Fig. 5. The interferogram obtained on the CCD of the interferometry will be analyzed by a software to get the wavefront. The simulation of the test system in Figs. 6 and 7 is carried out in Zemax to evaluate the system's ability to inspect medium and low spatial wavefront errors. Lens data are shown in Table 2.

The PV of wavefront of the test plan with concave mirror is 0.0237λ and RMS is 0.0044λ, which satisfy the required specification; so the test plan with concave mirror gives better performance than the former.

In order to formulate machining and assembly plans of the optical elements, tolerances analyses of the test system are performed in Zemax. Besides, tolerances analyses also help evaluate the performance of test plans dealing with wavefront of different degrees of distortion. In some cases of designing compensated lenses, some test systems with good design performance often fall into the dilemma that the fabrication and assembly process introduce some errors which lead to damaged result. To avoid the phenomena, Zemax provides the function of tolerance to analyze the effect of the error of radius of the lens, irregularity of surfaces, distance between optical components, refraction index, tilt, decentration of the optical surface, and so on, with corresponding operands such as TFRN, TIRR, TTHI, TIND, TSTX and TSDX. Firstly, the sensitivity mode is utilized to analyze the influence in RMS wavefront produced by the small change in the operands to simulate the real condition of optical elements fabrication and assembly process. In the beginning, loose restrictions are given, and then the restrictions are tightened according to the change in the wavefront RMS step by step, until the restrictions reach the limits of fabrication and assembly accuracy (Table 3) or the

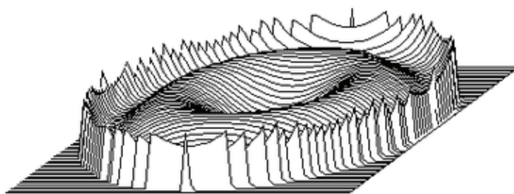

Fig. 3. Wavefront map of the test light back into the interferometer.

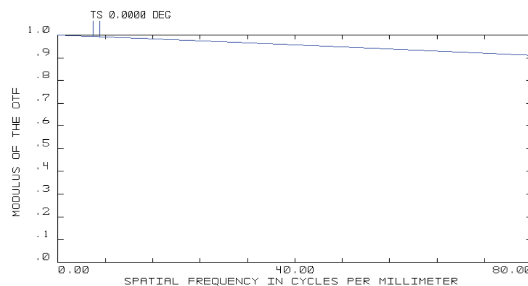

Fig. 4. MTF curves of the test system with plane mirror.

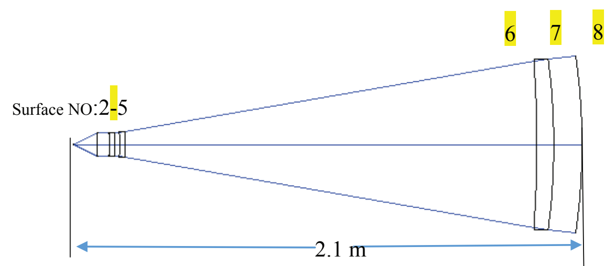

Fig. 5. Layout of the beam path of the test system with concave mirror.

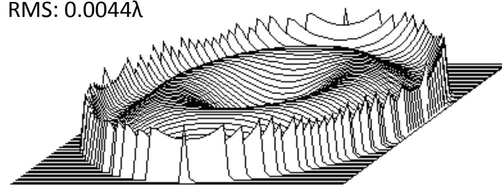

Fig. 6. Wavefront map of the test light back into the interferometer.

Table 2. Lens Data of the Test System with Concave Mirror (units: mm)

	Surf:Type	Radius	Thickness	Glass	Semi-Diameter
OBJ	Standard	Infinity	100.000000		0.000000
STO	Paraxial		50.000000		48.000000
2	Standard	–517.719061	20.000000	H-K9L	48.000000
3	Standard	Infinity	24.216063		48.703036
4	Standard	–258.094105	20.000000	H-K9L	49.633134
5	Standard	1118.329850	1700.062519		52.182348
6	Standard	–5000.000000	70.000000	H-K9L	346.808133
7	Standard	–2758.000000	116.863622		354.995866
8	Standard	–2621.366574	–116.863622	MIRROR	371.216419

Table 3. Fabrication and Assembly Accuracy of Optical Elements

Operand	Min	Start point	Comments
TFRN	1fringe	3 fringes	Curvature radius
TTHI	0.01 mm	0.05 mm	thickness
TEDX	0.02 mm	0.05 mm	Element decentration
TETX	5″	0.1°	Element tilt
TSDX	0.02 mm	0.05 mm	Surface decentration
TIRX	0.01 mm	0.05 mm	Surface tilt
TIRR	0.33 Fringe	0.5 Fringe	Surface irregularity
TIND		0.001, 3B	Refractive index

Table 4. Worst Offenders of the Tolerancing Operands in Sensitivity Analysis Mode

Worst offenders:					
Type			**Value**	**Criteria**	**Change**
TIND	4		–0.000500000	0.282780285	0.248019149
TIND	4		0.000500000	0.145717500	0.110956364
TETX	6	6	–0.002000000	0.132840425	0.098079289
TETX	6	6	0.002000000	0.132840425	0.098079289
TETY	6	6	–0.002000000	0.132840423	0.098079287
TETY	6	6	0.002000000	0.132840423	0.098079287
TFRN	5		2.000000000	0.096742782	0.061981645
TFRN	4		–2.000000000	0.095466488	0.060705352
TIRX	8		–0.05000000	0.089090460	0.054329324
TIRX	8		0.05000000	0.089090460	0.054329324

Table 5. Monte Carlo Analysis

Probability (%)	PV/λ ≤
90	0.255003427
50	0.170598057
10	0.074742092

Table 6. Tolerances Distribution Limited by the Real Fabrication and Assembly Accuracy

Surface	TFRN (fringe)	TTHI (mm)	TSDX/TSDY (mm)	TIRX/TIRY (mm)	TIRR (fringe)	Element	TEDX (mm)	TETX (degree)	TIND
2	±1	±0.05/25.25	±0.05	±0.05	±0.1	2	±0.05	±0.1	1B
3	±1	±1/9689.9	±0.05	±0.05	±0.1	4	±0.05	±0.05	1B
4	±2	±0.05/70	±0.05	±0.05	±0.3	6	±0.05	±0.002	
5	±2	±0.05/100	±0.05	±0.02	±0.3				
6	±0.5				±0.05				

Table 7. Worst Offenders of Tolerances of the Test Plan with Concave Retroreflector

Type			Value	Criteria	Change
TIRR	8		0.200000000	0.021506582	0.021291026
TIRR	8		−0.200000000	0.021361182	0.021145625
TETY	6	7	−0.003000000	0.014174723	0.013959166
TETX	6	7	−0.003000000	0.014174722	0.013959165
TETX	6	7	0.003000000	0.014174722	0.013959165
TETX	9	10	−0.003000000	0.014174150	0.013958593
TETX	9	10	0.003000000	0.014174150	0.013958593
TETY	9	10	−0.003000000	0.014174150	0.013958593
TETY	9	10	0.003000000	0.014174150	0.013958593
TIRY	9		−0.030000000	0.013687909	0.013472352

wavefront RMS performance meets the demand of the test system. Secondly, the Monte Carlo mode is applied to analyze the performance of the system with the combination of all the possible errors, which evaluate the real test result[13].

In the sensitivity mode, the test project with plane reflector cannot meet the requirement on wavefront RMS, as shown in Table 4. In the given processing, the class of refractive index of the glass used for the long focal length lens glass is 1B, whose refractive index varies in the range of ± 0.0005. But under this situation, the wavefront RMS increased by 0.24801, which is far greater than the requirement.

The Monte Carlo analysis stands for the estimation of actual performance of the test system. As shown in Table 5, the wavefront RMS is 0.255λ by the probability of 90%. As the PV value is often 6–8 times of the RMS value, the wavefront PV of this test plan is definitely $> 1/3\lambda$. Figure 8 shows the wavefront map of the test light with tolerances. Its PV is 1.9868λ, which is greater than the required PV 1/3λ. As a result, under the tolerance accuracy level (Table 6), the test system with plane retroreflector is not qualified for testing the long focal length lens.

The reason for this test system with a long optical path and flat mirror is the plane lens has poor ability

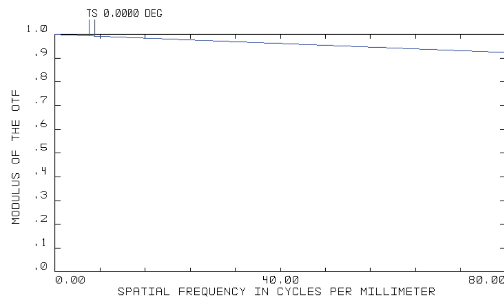

Fig. 7. MTF curves of the test system with concave mirror.

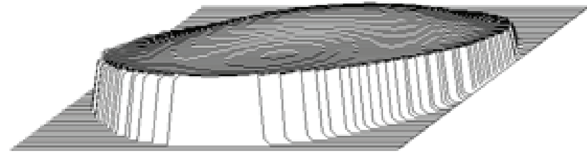

Fig. 8. Transmitted wavefront with tolerances of optical elements

to eliminate the spherical aberration produced by the long focal length lens with a very large aperture. The spherical aberration is proportional to the square of the aperture of lens, so the larger the lens' aperture, the greater the spherical aberration. As shown in Table 4, the error of refractive index has a great effect on the wavefront, because the spherical aberration is related to the refractive index. A tiny variation in the index leads to changes in the figure of the wavefront, but the plane mirror behind does not have enough ability to correct the spherical aberration. So for the system to work, an extremely accurate assembly and fabrication should be applied. However, it is always difficult and expensive to achieve that high precision.

Although the plan just needs a piece of small aperture compensated lens which would be fabricated easily, however it is a system with weak ability to correct spherical aberration. Especially when the deformation of the figure of the lens under test is far from the final acceptance requirements, the interferogram will be too intensive to be analyzed. So the test plan is inappropriate for inspecting the medium and low spatial wavefront errors of transmitted wavefront of the long focal length lens.

Analyses of tolerances of the test system with a large aperture concave mirror are also carried out in Zemax. Table 7 shows the worst offenders of tolerances. It can be seen from Table 8 that transmitted wavefront RMS is less than 0.0527 by the probability of 90%. Figure 9 shows the wavefront of the test light, whose PV is 0.2391λ. Thus the system meets the requirement of wavefront PV and RMS. The Zygo DynaFiz instantaneous interferometer is applicable for inspecting the medium and low spatial wavefront errors with carrier fringes mode in the total distance of 2.1 m. The shortened distance helps reduce the influence of the air disturbance and the vibration of the test platform.

As shown in Table 7, the most important tolerances are the tilt of the second compensated lens and the tested lens, generated during the assembly process. In

Table 8. Monte Carlo Analysis of the Test Plan with Concave Mirror

Probability (%)	PV/λ ≤
90	0.052747280
50	0.040837382
10	0.032675156

Table 9. Tolerances Demanding the Optical Elements in the Test plan with Concave Mirror

Surface	TFRN (fringe)	TTHI (mm)	TSDX/TSDY (mm)	TIRX/TIRY (mm)	TIRR (fringe)	Element	TEDX (mm)	TETX (degree)	TIND
2	±2	±0.05/20	±0.05	±0.05	±0.33	2	±0.05	±0.1	2B
3	±2	±0.05/24.21	±0.05	±0.05	±0.33	4	±0.05	±0.003	2B
4	±2	±0.05/20	±0.05	±0.05	±0.33	6	±0.05	±0.003	1B
5	±2	±0.05/1700.06	±0.05	±0.01	±0.33	8	±0.02	±0.05	
6	±2	±0.05/70	±0.05	±0.01	±0.05				
7	±2	±0.05/116.86	±0.05	±0.03	±0.33				
8	±2				±0.2				

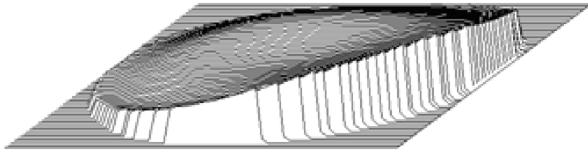

Fig. 9. Transmitted wavefront with tolerances of optical elements.

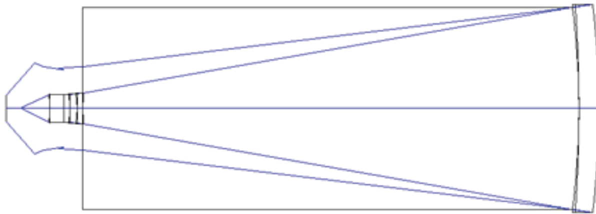

Fig. 10. Schematic of the ghost produced by the reflection of the rear surface of tested lens.

addition to component tilt, the surface tilt of the rear surface of the compensated lens and the front surface of the tested lens which are produced during the fabrication process also affect the wavefront RMS seriously. So those two tolerances should be up to the design speculations, while the other tolerances can be loosened in line with the assembly process to reduce cost and time. Especially, the requirement for the astigmatism of the large aperture concave mirror should be strict.

The reflective light from the rear surface of the tested lens may form spots on the CCD in the interferometer, which reduces the contrast of the interferogram. To analyze the influence of the ghost image, the rear surface is set as a mirror to reflect the test light back into the interferometer. It can be seen in Fig. 10 that the reflective light from the rear surface diverges into a large angle. When it reaches the CCD, the reflective light does not produce spots on the CCD. So the ghost image from the rear surface of tested lens does no harm on the test results.

In conclusion, the comparison of the two kinds of interferometric test of long focal length lens shows that the system with plane retroreflector has weak ability to correct the spherical aberration, and it demands high precision for the fabrication and assembly of the optical elements. Furthermore, when the deformation of the figure of the lens under test is far from the final acceptance requirements, the interferogram is too intensive to be analyzed. So the plane mirror system is not appropriate for the test during the process of lens fabrication. The system with concave mirror as reflector works for wider dynamic range of the figure of the lens. It does not need very high precision for the fabrication and assembly of the lens under test and compensated lenses, as shown in Table 9. And the estimation of transmitted wavefront RMS is $< 0.052\ \lambda$ by the probability of 90%. However, the disadvantage of the system is that the fabrication of the large aperture concave mirror is expensive and time-consuming. So the medium and low spatial wavefront errors of long focal length lens are tested by the traditional interferometric method with an instantaneous interferometer and we will process the related optical elements, including the concave mirror with large aperture and other compensated lenses and test the long focal length lens.

This work was supported by the National Natural Science Foundation of China under Grant No. 11104295.

References

1. T. G. Parham, T. J. McCarville, and M. A. Johnson, in *Proceedings of Optical Fabrication and Testing* OWD8 (2002).
2. R. Zhang, “Studies on the high-accuracy wavefront test techniques of optical components in ICF” PhD. Thesis (Sichuan University, 2003).
3. J. Zhang, X. Zhang, Z. Zhang, and L. Zhang, Opt Prec. Eng. **20,** 492 (2012).
4. H. Zheng, H. Rao, X. Rao, W. Jiang, and J. Yang, Acta Opt. Sin. **29,** 3385 (2009).
5. C. Hou, J. Xu, J. Bai, and G. Yang, Opt. Electron. Eng. **34,** 61 (2007).
6. Y. Nakano and K. Murata, Appl. Opt. **24,** 3162 (1985).
7. D. R. Neal, J. Copland, and D. Neal, Proc. SPIE **4779,** 148 (2002).
8. J. Yue, Z. Lu, H. Liu, and H. Zhang, J Opt. Electron. Laser **21,** 25 (2010).
9. J. Xu, “Research on technique of high resolution wavefront interferometric measuring” PhD. Thesis (China Academy of Engineering Physics, 2006).
10. E. L. Church, in *Proceedings of 31st Annual Technical Symposium* (1988).
11. S. Li and L. Lin, *Optical Design Manual* (Beijing University of Science and Technology Press, 1990).
12. J. H. Pan, *The Design, Manufacture and Test of the Aspherical Optical Surfaces* (Science Press, 1994).
13. L. Liu, X. Zhang, and Y. He, Laser Infrared **05**, 496 (2010).